ACS Chemical Neuroscience

Research Article

pubs.acs.org/chemneuro

Ascorbate Protects Neurons against Oxidative Stress: A Raman Microspectroscopic Study

Abhaya Dutta,[†,‡] Rekha Gautam,[‡] Sreejata Chatterjee,[†] Freek Ariese,[‡,∥] Sujit Kumar Sikdar,[*,†] and Siva Umapathy[*,‡,§]

[†]Molecular Biophysics Unit, [‡]Department of Inorganic and Physical Chemistry, and [§]Department of Instrumentation and Applied Physics, Indian Institute of Science, Bangalore 560012, India

[∥]LaserLaB, Faculty of Sciences, VU University Amsterdam, 1081 HV Amsterdam, The Netherlands

Supporting Information

ABSTRACT: Oxidative stress due to excessive accumulation of reactive oxygen or nitrogen species in the brain as seen in certain neurodegenerative diseases can have deleterious effects on neurons. Hydrogen peroxide, endogenously generated in neurons under normal physiological conditions, can produce an excess of hydroxyl radical via a Fenton mediated mechanism. This may induce acute oxidative injury if not scavenged or removed effectively by antioxidants. There are several biochemical assay methods to estimate oxidative injury in cells; however, they do not provide information on the biochemical changes as the cells get damaged progressively under oxidative stress. Raman microspectroscopy offers the possibility of real time monitoring of the chemical composition of live cells undergoing oxidative stress under physiological conditions. In the present study, a hippocampal neuron coculture was used to observe the acute impact of hydroxyl radicals generated by hydrogen peroxide in the presence of Fe^{2+} (Fenton reaction). Raman peaks related to nucleic acids (725, 782, 1092, 1320, 1340, 1420, and 1576 cm^{-1}) showed time-dependent changes over the experimental period (60 min), indicating the breakdown of the phosphodiester backbone as well as nuclear bases. Interestingly, ascorbic acid (a potent antioxidant) when cotreated with Fenton reactants showed protection of cells as inferred from the Raman spectra, presumably by scavenging hydroxyl radicals. Little or no change in the Raman spectra was observed for untreated control cells and for cells exposed to Fe^{2+} only, H_2O_2 only, and ascorbate only. A live−dead assay study also supported the current observations. Hence, Raman microspectroscopy has the potential to be an excellent noninvasive tool for early detection of oxidative stress that is seen in neurodegenerative diseases.

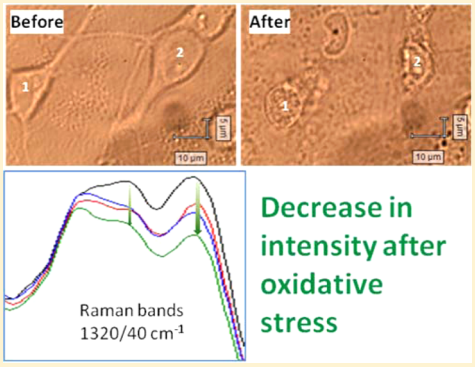

KEYWORDS: *Raman spectroscopy, hippocampal neuron, oxidative stress, neurodegenerative disease, reactive oxygen species*

Oxidative stress has been suggested to play a critical role in a number of neurodegenerative diseases including Parkinson's, Alzheimer's, and Huntington's disease.[1,2] In the case of Alzheimer's disease, increasing evidence points at the role of oxidative stress in neuronal degeneration. Loss of memory and cognition are common signs of Alzheimer's disease wherein deposition of β-amyloid plaque and loss of neurons are observed in some brain areas especially in the hippocampus.[1,2] Reactive oxygen species, which includes free oxygen radicals like superoxide anion, hydroxyl radical, as well as nonradical oxidants like hydrogen peroxide that are generated by normal cellular metabolism, play a major role in oxidative stress. Hydrogen peroxide synthesized in the cells at normal physiological concentration does not harm cells, but rather acts as an intracellular signaling molecule for cell survival by activating or inactivating proteins related to cell survival.[3] However, in the presence of transition metals like copper or iron, it produces hydroxyl radicals via a Fenton mediated mechanism. These hydroxyl radicals are known to produce oxidative injury in cells by inducing oxidation of major cellular components (lipids, proteins, and nucleic acids) if the antioxidant defense system is inadequate.[4−7] In certain conditions like brain ischemia, the concentration of hydrogen peroxide may reach up to 200 μM, and in the presence of endogenous Fe^{2+} it can generate an excess of hydroxyl radicals that may not get scavenged effectively by antioxidants in situ and can induce damage to both neurons and astrocytes.[8−10]

There are several antioxidant enzymes such as superoxide dismutase, catalase, peroxidase, as well as low molecular weight antioxidants such as glutathione, NADPH, *N*-acetyl cysteine, vitamin E, ascorbic acid, retinoic acid, and lipoic acid that have been demonstrated to protect against oxidative injury in several neurodegenerative disease conditions.[1,6] Among these, ascorbic acid has a better distribution in the brain especially in the

Received: April 2, 2015
Revised: July 13, 2015
Published: August 3, 2015

DOI: 10.1021/acschemneuro.5b00106
ACS Chem. Neurosci. 2015, 6, 1794−1801

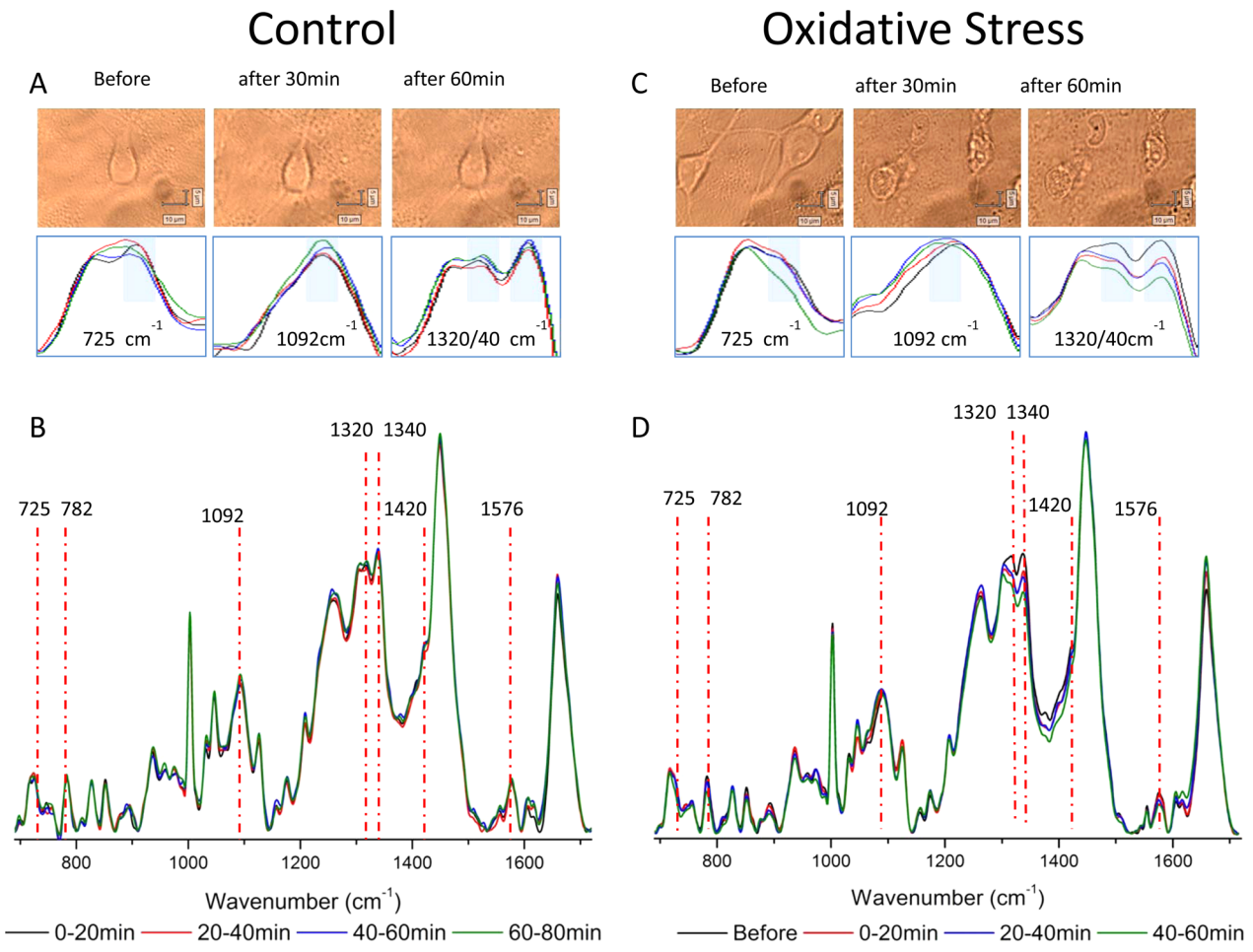

Figure 1. (A) White light images of live hippocampal neuronal cell (control) before and after 30 and 60 min. (B) Raman spectra recorded from the same cell as in (A) before (black), at 0−20 min (red), 20−40 min (blue), and 40−60 min (green) at fingerprint region (690−1720 cm^{-1}). Important DNA peaks are marked (725, 782, 1092, 1320, 1340, 1420, and 1576 cm^{-1}). Four Raman peaks/bands (725, 1092, 1320, and 1340 cm^{-1}) are highlighted in the insets. (C) White light image of neuronal cell before, after 30 and 60 min of hydroxyl radical treatment. (D) Raman spectra recorded from the same oxidatively stressed cell as in (C) before (black) and at 0−20 min (red), 20−40 min (blue), and 40−60 min (green) after treatment. The same Raman peaks/bands are highlighted in the insets.

hippocampus and amygdala.[11] Thus, it may provide a better defense in these brain areas against oxidative injury.

Depending on the extent of oxidative stress, several assay methods have been developed to monitor cells/tissues under oxidative stress. However, these assay techniques use a large number of cells and the cells need to be sacrificed (for fixation, staining). Live cell fluorescence microscopy is another commonly used technique, but for this technique external tagging molecules are required, which may interfere with cell health.

Raman spectroscopy enables a label free, noninvasive, and continuous biochemical analysis of living cells under normal physiological conditions. Raman spectroscopy is based on the principle of inelastic scattering of light upon interaction with the molecules and provides a fingerprint of the molecular composition of the sample under investigation.[12−16] The Raman spectrum is sensitive to changes in the structure and the chemical environment of the molecule. Any change in these characteristics of biomolecules, due to oxidative attack or any other reason, gets reflected in the Raman spectra, enabling the development of diagnostic markers based on Raman spectroscopy.

Raman microspectroscopy, a combination of spectroscopy and microscopy, incorporates the benefits of both the high spatial resolution of optical microscopy and the chemical information by Raman spectroscopy. Using this technique, a number of studies has been carried out on various cell lines where oxidative stress as well as apoptosis was induced by different chemical agents such as glyoxal, Fenton reagent, etoposide, ricin, sulfur mustard, and Triton X 100.[17−22] By exposing cells to room temperature (RT-induced apoptosis), cell death stages have been monitored with Raman spectroscopy.[23] However, in most of these studies, various cancer cell lines were used with focus on cancer research, or yeast cells which have very different Raman spectra compared to mammalian cells. Recently, to evaluate the compatibility of various nanoparticles in biomedicine, the stressful effect of silver nanoparticles on human mesenchymal stem cells has been demonstrated with Raman microspectroscopy.[24] Raman spectroscopy studies have been performed on neuronal stem cells to identify the various stages of differentiation.[25] However, the application of Raman spectroscopy to mature neurons and oxidatively stressed neurons, which are associated with neurodegenerative diseases, has not yet been reported.

DOI: 10.1021/acschemneuro.5b00106
ACS Chem. Neurosci. 2015, 6, 1794−1801

To explore this dimension of neurotoxicology, a rat hippocampal neuronal culture was used as a cellular oxidative injury model in the present study. The advantage of using a primary cell culture is that these are more suitable than an immortal cell line as their properties are more comparable to those of in vivo cells.[26] Herein, the effect of hydrogen peroxide in the presence of Fe^{2+} on rat hippocampal neurons was studied to elucidate the biochemical changes in neurons induced by oxidative stress and to understand the underlying mechanisms of neurodegenerative diseases including Alzheimer's. Furthermore, the protective role of ascorbate in oxidative stress was analyzed by cotreating with ascorbate neuronal cultures that were oxidatively stressed with hydrogen peroxide and Fe^{2+}.

RESULTS AND DISCUSSION

Real Time Monitoring of Hippocampal Pyramidal Cells under Physiological Conditions. Figure 1A depicts the white light image of the neuronal cell kept under normal physiological conditions before treatment, at 30 min, and at 60 min post treatment (the same cell for which Raman spectra were recorded simultaneously). No or minimal morphological changes are observed in the cell until the end of the experimental period.

Corresponding Raman spectra recorded from the same neuronal cell in the lower wavenumber region (690−1720 cm^{-1}) are shown in Figure 1B. Raman spectra of neuronal cell consist of contributions from all cellular chemical components such as protein, DNA/RNA, lipid, and carbohydrates as summarized in Table 1. In the average Raman spectrum of a neuronal cell, the contributions from the nucleic acids are clearly visible. The important Raman bands of nucleic acids correspond to the nuclear bases such as 725 cm^{-1} (adenine), 782 cm^{-1} (cytosine, uracil, thymine), 1320 cm^{-1} (guanine), 1340 cm^{-1} (adenine, guanine), 1420 cm^{-1} (adenine, guanine), and 1576 cm^{-1} (adenine, guanine) and to the phosphate-sugar backbone vibrations at 1092 cm^{-1} (PO_2^-). Proteins have intense peaks at 1005 cm^{-1} (phenylalanine), 1200−1300 cm^{-1} (amide III), 1320 and 1340 cm^{-1} (C−H deformations), and 1665 cm^{-1} (amide I). Lipid peaks are observed at 1301 cm^{-1}, 1449 cm^{-1} (C−H deformations) and 1660 cm^{-1} (C═C stretching). All these three major cellular components have overlapping contributions in the presented fingerprint zone (690−1720 cm^{-1}).

For control cells, no significant change was observed in the average intensity in any of the Raman peaks recorded at 0−20 min, 20−40 min, 40−60 min and 60−80 min as shown in Figure S2A (Supporting Information). All important peaks are marked on the averaged spectra at different time points in Figure 1B.

Effect of Hydroxyl Radical on Neuronal Cells. To generate oxidative stress on neuronal cells, 0.2 mM $FeSO_4$ and 0.2 mM H_2O_2 were added together to get a maximum yield of 0.2 mM hydroxyl radical in the incubation medium. As mentioned earlier, the concentration of H_2O_2 can reach this level in global brain ischemic conditions.[9] Similarly, $FeSO_4$ has a broad distribution in several brain parts and the amount of $FeSO_4$ present in the hippocampus lies in the same range as we have used in the present study.[27,28]

To ensure that the resultant stress is due to hydroxyl radical and not because of Fe^{2+} or H_2O_2 per se, two different sets of experiments were conducted and the results are shown in Figure S1. The cells treated with only Fe^{2+} showed no significant alteration in the intensity of the Raman peaks except

Table 1. [a]

wavenumber (cm^{-1})	spectral assignments
715	C−C−N symmetric stretching in phosphatidylcholine
725	nucleic acid (A)[b]
757	Symmetric ring breathing in tryptophan
782−788	782-nucleic acid (C,T, U-ring breathing);[b] 788-DNA:backbone O−P−O stretching
810	RNA:backbone O−P−O stretching
829	Proline, hydroxyproline-collagen; out-of-plane ring-breathing in tyrosine
850	C−C stretch in proline (collagen); ring breathing (tyrosine); C−O−C stretching (glycogen, polysaccharides)
877	C−C−N symmetric stretching (lipids); C−O−C ring (carbohydrate)
901	C−C stretch: β-structure
920	C−C stretch of proline ring/glucose/lactic acid
938	C−C stretch: α-helix; collagen
1005	symmetric ring breathing mode of phenylalanine
1031	C−H in plane bending of phenylalanine; carbohydrates (glycogen)
1091	DNA backbone: PO_2^- stretching
1127	C−N stretch: proteins; C−C stretch: lipids
1156	C−C stretch: carotenoids; C−C/C−N stretch: proteins
1204−1209	C−C_6H_5 stretch: phenylalanine , tryptophan; CH_2 wagging, hypro, tyr, phe
1220−1310	amide III: mostly NH in-plane bending and CN stretching
1257	nucleic acid (A,C)[b]
1301	CH_2 twist/ wag/ deformation: lipids; amide III α-helical structures
1320	CH_2 CH_3 twisting; proteins/lipids nucleic acid (G)[b]
1340	Nucleic acid (A,G);[b] protein CH_2 deformation
1375	Nucleic acid (A,G, T)[b]
1420	Nucleic acid (A,G)[b]
1440	CH_2 bending: lipids
1449	CH_2 bending: proteins
1524	C═C stretch: carotenoids
1552	N−H bending and C−N stretch in proteins (amide II)
1576	nucleic acid (A,G)[b]
1607	C═C phenylalanine, tyrosine
1617	C═C tyrosine, tryptophan
1635−1680	amide I: predominantly C═O stretch in proteins

[a]Band assignments for the Raman spectra are from refs 17, 19, 21, and 24. [b]C = cytosine, *T* = thymine, A = adenine, G = guanine, U = uracil.

the 1420 cm^{-1} band at 40−60 min. Similarly, the other group of cells treated with only H_2O_2 also showed very little change, with a significant decrease in intensity of only the 1340 and 1420 cm^{-1} peaks at later time points. These results are in line with literature reports showing no or much slower effects for Fe^{2+} only and H_2O_2 only. Regarding $FeSO_4$ induced toxicity at the present concentration, Alcântara et al. have shown that there is no cytotoxic effect even after 24 h of treatment with the same concentration to a central nervous system cell line.[29] However, Liu et al. have shown significant cell death in hippocampal slice culture when treated with 0.2 mM $FeSO_4$ for 24 h.[30] Regarding H_2O_2 induced cytotoxicity, Hardaway et al. have shown that it does not produce any significant cell death up to 0.4 mM even after 24 h incubation.[31] Ammar et al. have also demonstrated that 0.5 mM H_2O_2 did not produce any trabecular meshwork cell death when incubated for 24 h in medium.[39]

Figure 1C shows the white light image of a neuronal cell before and after treatment with $FeSO_4$ and H_2O_2 at 30 and 60

DOI: 10.1021/acschemneuro.5b00106
ACS Chem. Neurosci. 2015, 6, 1794−1801

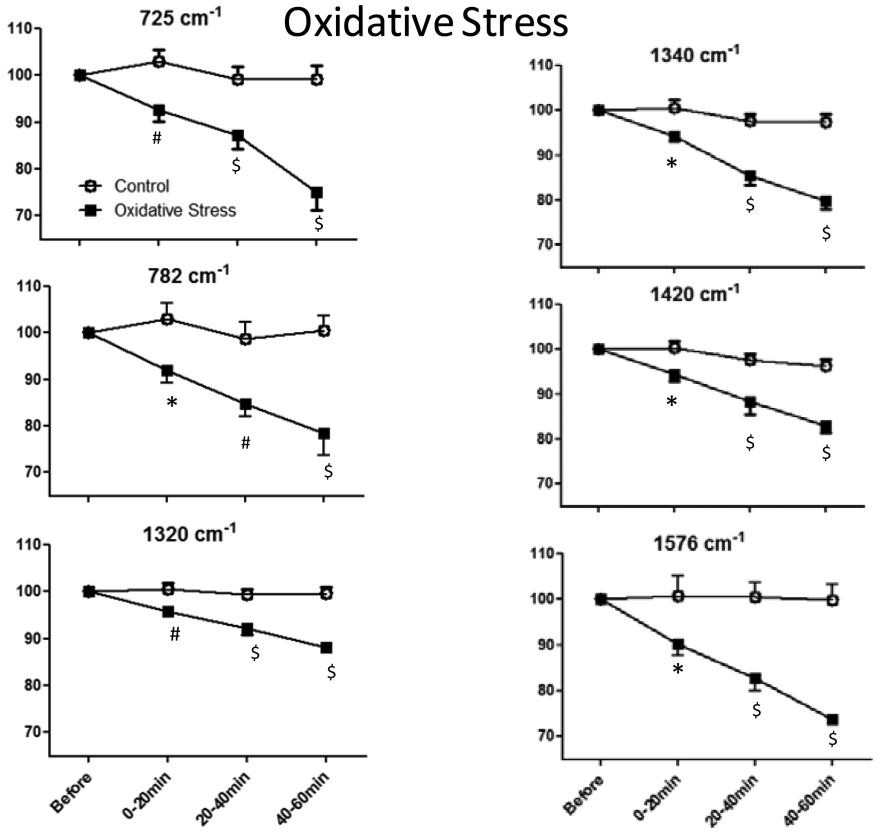

Figure 2. Line graphs showing a time dependent decrease in intensity of the 725, 782, 1320, 1340, 1420, and 1576 cm^{-1} peaks obtained from the oxidatively stressed group (squares). The mean ± SEM values are significantly different from those of the control group (circles) when compared to the time matched control value. Two-way ANOVA; $^{*}P < 0.05$, $^{\#}P < 0.01$, $^{\$}P < 0.001$.

min, and Raman spectra were recorded from the same cell, as was also done for the control. Morphological changes were observed after 30 min of hydroxyl radical treatment as shown in Figure 1C. Cells became more round in shape, and structures became visible inside the cell. The cell nucleus appeared to be fragmented and spread all over the cytoplasm of the cell. While only two to three cells are shown in the image, the majority of the cells in the plate underwent similar morphological changes after treatment.

Figure 1D depicts the average Raman spectra recorded from the same neuronal cell shown in Figure 1C, before as well as after hydroxyl radical treatment at the indicated time points. Peaks that showed progressive significant changes in intensity are marked in the original spectra. The peaks that showed most significant changes under oxidative stress are 725, 782, 1092, 1320, 1340, 1420, and 1576 cm^{-1}. There was a progressive decrease in the intensity of these peaks with time except the 1092 cm^{-1} peak. This decrease in intensity was observed at 0−20 min ($P < 0.05$); however, at 20−40 min it was more pronounced ($P < 0.001$) and at 40−60 min a further decrease ($P < 0.001$) was observed as shown in Figure S2B (one-way ANOVA followed by Newman−Keuls test). After 60 min of oxidative stress treatment, the 725 cm^{-1} peak intensity decreased by 25%, the 782 cm^{-1} peak by 27%, the 1320 cm^{-1} peak by 12%, the 1340 cm^{-1} peak by 19%, the 1420 cm^{-1} peak by 17%, and the 1576 cm^{-1} peak by 28%. These changes are similar to earlier observations.[32] In comparison to the control group, the progressive decrease in the peak intensities was significant as shown in Figure 2 ($P < 0.05$, two-way repeated measures ANOVA). Similar concentration dependent intensity changes in the DNA related peaks has been described in human sperm treated with varying concentrations of Fenton reagent to induce nuclear DNA damage.[18] Nakamura et al.[7] have also shown the presence of aldehydic lesions in extracted DNA from HeLa cells exposed to low and high concentrations of hydrogen peroxide for 15 min. Studies by Henle et al.[5] reported that hydroxyl radical generated from Fenton reactions produces cleavage in DNA in a sequence specific manner. Similar spectral changes were reported earlier in oxidatively stressed lung fibroblast cells, although a kinetic study was not done.[17] Apart from oxidative stress, apoptosis induced by thermic stress, chemotherapeutic, and pharmaceutical substances producing similar changes in nucleic acid peaks have been reported previously.[19,22,23,32,33] Further, Fenton reagent is known to induce apoptosis in various cells including neuronal cells.[10,34−38] For the phosphodioxy group vibration at 1092 cm^{-1}, there was no significant decrease in the peak intensity, but a shift of this peak toward lower wavenumber was observed after 40 min as shown in Figure 3 ($P < 0.05$, two-way repeated measures ANOVA). This can be related to cleavage of the phosphodiester bond in the phosphate backbone.[20]

There was very minimal or no change in lipid related peaks as the spectra were mainly recorded from the nuclear part of the cells. However, in the yeast cell study reported earlier, mainly changes in the lipid peaks were observed.[4] In the future, we intend to record spectra from the cytoplasmic part of the cells to monitor lipid related changes. In a preliminary study, we observed that the Raman spectra recorded from the cytoplasmic part of neurons had strong signatures of lipids (spectra not shown). Peaks related to proteins were prominent

DOI: 10.1021/acschemneuro.5b00106
ACS Chem. Neurosci. 2015, 6, 1794−1801

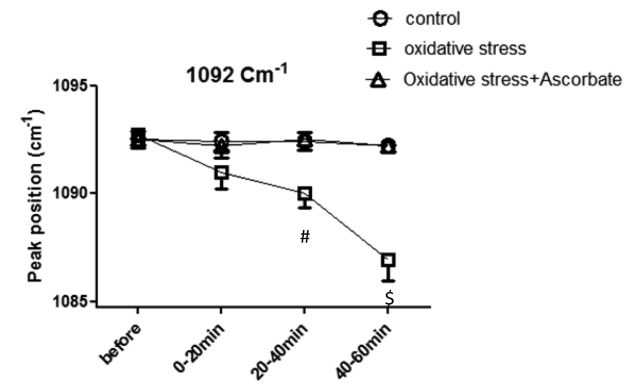

Figure 3. Line graph showing time dependent wavenumber shift in the 1092 cm^{-1} peak. The mean ± SEM values obtained from stressed cells are significantly different but not those from the antioxidant cotreated cells when compared to the time matched control value. Two-way ANOVA; $^{\#}P < 0.01$, $^{\$}P < 0.001$.

in the control as well as in the stressed cells, although the peaks related purely to protein did not show much change until the end of the experimental period. The 1320 and 1340 cm^{-1} peaks have contributions from protein and nuclear bases, so the observed changes must be due to changes in the nucleobase levels. In the literature, protein peaks did not alter much in glyoxal treated (24 h) cells.[17]

Protective Effect of Ascorbate from Hydroxyl Radical Induced Oxidative Stress. In a subsequent set of experiments the protective influence of ascorbate was investigated. To eliminate the possibility of any cellular changes induced by ascorbate, a separate group of cells was treated with ascorbate only. Results obtained from this group are shown in Figure S3A. Most averaged Raman peaks showed little or no change in intensity; significant changes were observed only for the 1340 and 1420 cm^{-1} bands at later time points. Thus, there might be a possibility of some level of damage due to delayed oxidative stress by oxidized ascorbate.

Figure 4A shows that the morphology of the neuronal cells remained intact and did not undergo significant changes when ascorbate and hydroxyl radicals were applied together. Figure 4A shows the same cell before treatment, and 30 and 60 min after treatment. The observed cell maintained similar morphological features without any shape change, and no evidence of opacity or nuclear fragmentation was seen. Averaged Raman spectra recorded from the same cell before treatment and 0−20, 20−40, and 40−60 min after cotreatment with hydroxyl radical and ascorbate are shown in Figure 4B.

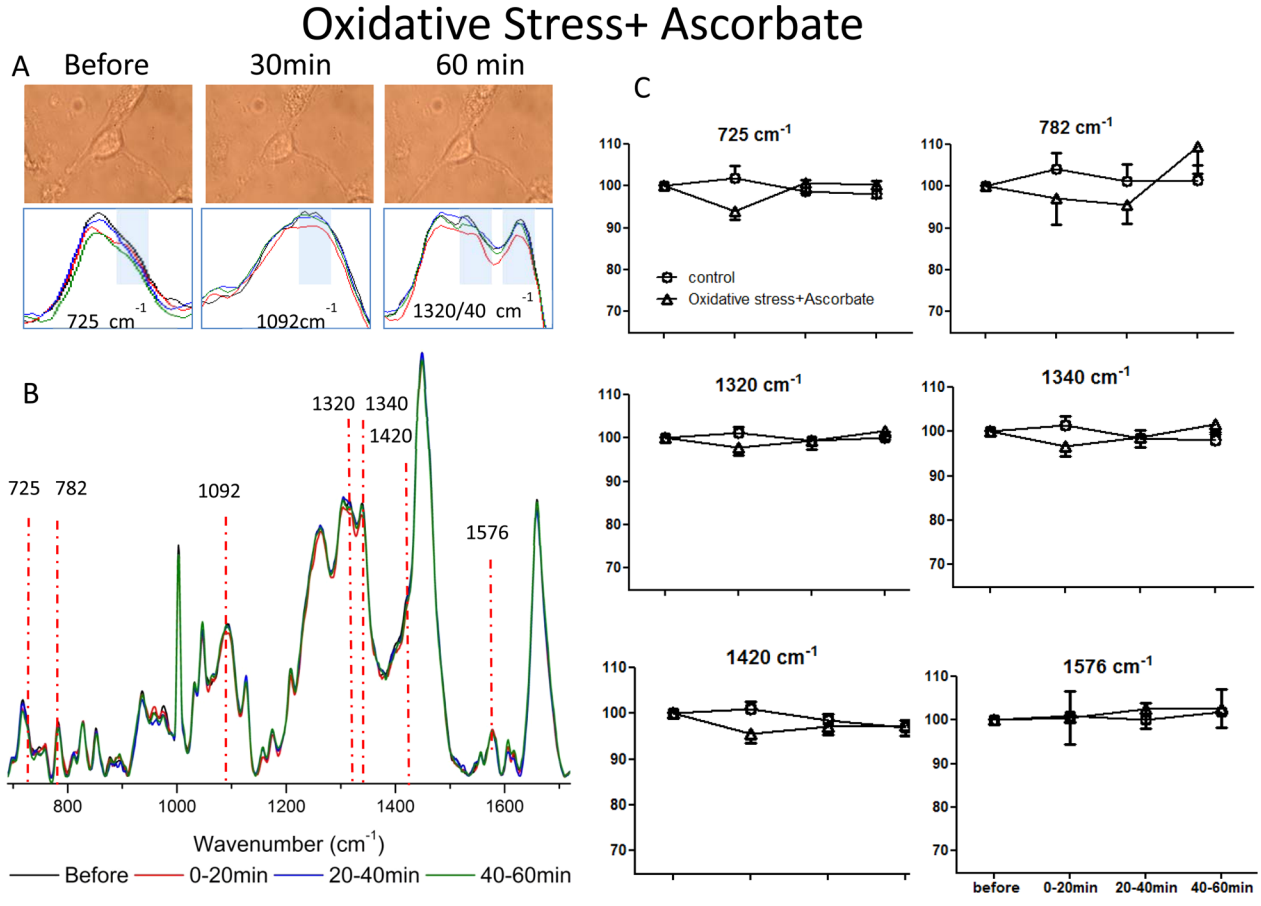

Figure 4. (A) White light image of neuronal cell before, after 30 and 60 min of antioxidant cotreatment in oxidatively stressed neurons. (B) Raman spectra recorded from the same cell before (black), at 0−20 min (red), 20−40 min (blue), and 40−60 min (green) at fingerprint region (690−1720 cm^{-1}). Important peaks are marked (725, 782, 1092, 1320, 1340, 1420, and 1576 cm^{-1}). Four Raman peaks/bands (725, 1092, 1320, 1340 cm^{-1}) are highlighted in the inset. (C) Line graphs show the time dependence of the intensity of the 728, 782, 1320, 1340, 1420, 1576 cm^{-1} peaks obtained from antioxidant cotreatment group (triangles). The mean ± SEM values are not significantly different from those of the control group (circles).

DOI: 10.1021/acschemneuro.5b00106
ACS Chem. Neurosci. 2015, 6, 1794−1801

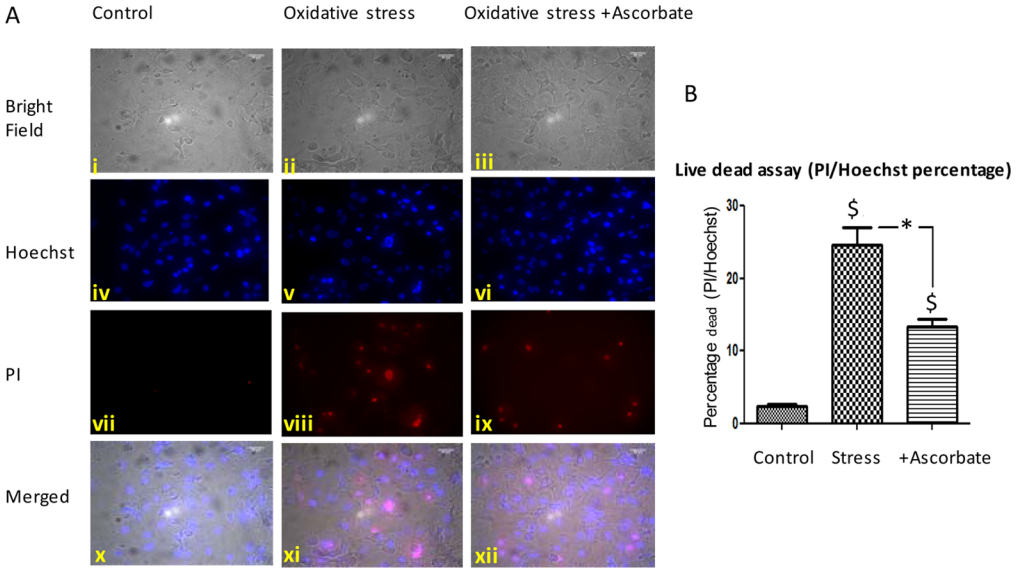

Figure 5. (A) White light and fluorescence images of control, stressed, and antioxidant cotreated cells. First row (i–iii) represents the white light, second row (iv–vi) represents the Hoechst positive, third row (vii–ix) represents the PI positive, and fourth row (x–xii) represents the merged (both Hoechst and PI positive) cells from each group. (B) Bar graph showing that the number of dead cells (in terms of percentage of PI positive cells) in the oxidatively stressed group was significantly greater than that in the control group; however, antioxidant cotreatment with ascorbate of oxidatively stressed cells shows protection ($P < 0.05$, one-way ANOVA). $^{*}P < 0.05$ when compared to the stressed group, $^{\$}P < 0.001$ when compared to the control group.

There was no significant change in average intensity in any of the Raman peaks, as shown in Figure S3B. In comparison to the control group, the averaged peak intensities were not significantly different as shown in Figure 4C ($P > 0.05$, two-way repeated measures ANOVA). Also, contrary to the data shown in Figure 3 for the nonprotected cells, the peak shift around 1092 cm^{-1} was not observed in this group (Figure 3; $P > 0.05$, two-way repeated measures ANOVA). Ascorbate protects nucleic acids from being oxidized in the presence of Fenton reagent, probably by scavenging hydroxyl radical generated by the Fenton reagent as reported earlier by Chang et al.[4]

Effect of Hydroxyl Radical/Antioxidant Cotreatment on Cell Viability. Figure 5A shows that the cells that were stained with propidium iodide (PI) have a compromised plasma membrane. PI positive cells occur more in hydroxyl radical treated and ascorbate cotreated cells than control; however, the counts are much lower for ascorbate cotreated cells than for hydroxyl radical treated cells. In the control group, PI positive cells amounted to only 2.4% but it was 24.7% in hydroxyl radical treated cells and 13.4% in ascorbate cotreated cells as shown in Figure 5B. The results show that in the oxidatively stressed group the cell viability decreased significantly in comparison to the control group, however the ascorbate cotreated cells showed better survival ($P < 0.05$, one-way ANOVA followed by Dunnett's test) as reported earlier.[11,39] In the oxidatively stressed group, neuronal cell death was comparatively more abundant than that of astrocytes when observed under the microscope. This could be due to higher susceptibility of neurons to oxidative injury in comparison to astrocytes, in agreement with a similar observation reported earlier by Terashvili et al.[10]

CONCLUSION

The results of the present study indicate that Raman microspectroscopy can detect very minute biochemical changes (decreased intensity of the DNA related peaks) in a single neuron already at 20 min which continued progressively up to 1 h (experimental period) of acute oxidative stress as seen in the case of ischemic reperfusion condition or global ischemia of the brain.[9] However, ascorbate was able to partially protect the DNA molecules, probably by scavenging the hydroxyl radicals. Additionally, the live–dead assay data obtained from fluorescence microscopy showed that cell death happens in a very slow or delayed fashion (only 25% after 1 h) when cells are under oxidative stress. Using Raman microscopy, the biochemical changes occurring at earlier time points could also be observed.

METHODS

Chemicals and Solutions. Ascorbate, ferrous sulfate, and all other chemicals for HEPES buffer preparation were obtained from Sigma Chemical Company, St. Louis, MO. Hydrogen peroxide was obtained from SDFCL, Mumbai, India. NucBlue and propidium iodide were procured from Invitrogen, Carlsbad, CA.

Network Culture of Hippocampal Neurons. Cultures were prepared from 1–3 day old rat pups (Wistar). The animals were killed by decapitation, and the brains were placed in ice-cold phosphate-buffered saline supplemented with glucose (30 mM) and 1% antibiotic–antimycotic. Cuts were made to separate the brain hemispheres from the olfactory lobe and the cerebellum. Next, a diagonal cut was made between the anterio-medial tip and the postero-lateral end of the brain hemispheres, exposing the cut hippocampus tucked inside the brain hemisphere medially. This excluded the dentate gyrus of the hippocampus. The hippocampi were dissected out and incubated with papain (20 U/mL) at 37 °C for 30 min. After draining papain, fresh medium was added and the suspension was gently triturated with a fire polished Pasteur pipet in order to avoid cell death by mechanical injury. The suspension was then filtered through a fine mesh and centrifuged at 1000 rpm for 5 min. The supernatant was discarded, and fresh medium was added in which the cells were resuspended and plated onto MgF_2 (magnesium fluoride) coverslips coated with 0.2 mg/mL poly-D-lysine. The culture medium used was DMEM F12 HAM supplemented with N1, 10% fetal bovine serum, and 1% antibiotic–antimycotic. The neurons were fed twice a week by

DOI: 10.1021/acschemneuro.5b00106
ACS Chem. Neurosci. 2015, 6, 1794–1801

removing half the medium and replacing it with fresh medium. After 3−4 days, 20 μM cytosine-β-D-arabinofuranoside was included in the medium to prevent glial cell overgrowth. The cells were grown for 6−7 days. The Institute's ethical committee approved the animal experiments described above.

Incubation of Cells with Hydroxyl Radical or Antioxidant + Hydroxyl Radical. Before performing Raman experiments, the culture coverslips were washed two to three times with HEPES buffer solution containing (in mM) NaCl 135, KCl 2.5, $CaCl_2$ 1.5, $MgCl_2$ 1.0, HEPES 5, D-glucose 10, to remove the medium and phenol red. The cells were incubated in the same buffer in a cell incubation chamber (from Okolab) on the microscope stage. After recording the control spectra (before hydroxyl radical treatment) for 20 min, the incubation buffer was replaced with the same buffer containing 0.2 mM $FeSO_4$ and 0.2 mM H_2O_2 to yield the same concentration of hydroxyl radical in the medium. Following the incubation, spectra were recorded for 60 min after treatment from the same cells from which control spectra were recorded earlier (n = 24). To exclude any time dependent effects on live cells, control (n = 22) experiments were conducted without any treatment for the same time. In the antioxidant cotreatment group (n = 8, live cell until the end of experiment), control or before treatment spectra were recorded as described above, followed by ascorbate (as antioxidant, 1 mM) cotreatment with hydroxyl radical. Immediately after cotreatment, spectra were recorded for the same duration as the control group and the hydroxyl radical treated group.

Incubation of Cells with Fe(II), H_2O_2, and Ascorbate Alone. To exclude any possible effects of Fe(II) (n = 8), H_2O_2 (n = 8), or ascorbate (n = 7) alone, three different control groups were separately incubated and Raman spectra were recorded in the same way, before and after incubation.

Raman Spectroscopy. Raman spectra were recorded using a commercial Renishaw (InVia) Raman microspectrometer equipped with a 785 nm line focus laser, 1200 lines/mm grating, and a thermoelectrically cooled charge-coupled device (CCD) detector. Before recording the spectra from the sample, the calibration of the system was checked with the 520.5 cm^{-1} line using a silicon reference. A water immersion objective lens, 63× (NA = 0.9), was used to focus the excitation laser beam onto the samples and to collect the backscattered Raman signals. Power at the sample was ∼15 mW. The system was controlled via Renishaw WiRE 3.2 software, which also controls the microscopic stage movement. All spectra were acquired for 5 s, and for each spectrum 10 scans were coadded. For each experiment, from each plate, two to three cells were considered (x and y coordinate of each cell was fixed). From each cell, six to eight Raman spectra were recorded, predominantly from the nucleus (total measurement time ∼ 20 min for all cells). This was done before and until 60 min after exposure to oxidative stress, with or without antioxidant cotreatment. Spectra recorded in each 20 min interval from each cell were separately averaged to observe the time dependent changes.

Data Preprocessing. The cosmic ray interference removal from the Raman spectra was done using Renishaw WiRE 3.2 software just after acquiring the spectrum. Averaged spectra obtained from each 20 min of recording from each cell were then background subtracted, baseline corrected (multipoint baseline), smoothed (Savitzky-Golay, 10 points), and normalized to the intensity of the 1441 cm^{-1} peak to eliminate the influence of inter/intraspectral variability using Origin Software.

Live Cell Staining for Cell Viability. To corroborate the findings from the Raman experiments, cell viability was checked by propidium iodide (PI)/NucBlue staining of control, hydroxyl radical, and ascorbate (cotreated with hydroxyl radical) treated sister cultures. Cultures exposed to hydroxyl radicals and ascorbate cotreatment, as mentioned above, were washed with HEPES buffer solution after 1 h (as above). The cells were then treated briefly for 15 min with PI (30 μg/mL) in HEPES buffer solution followed by a brief wash and incubation in NucBlue (2 drops/mL) for approximately 15 min (until a blue color developed) before imaging using a Leica DMI 6000B Live Imaging system. NucBlue is a Hoechst 33342 dye which binds to the A-T sites in the minor groove of double stranded DNA, and its presence is indicated by blue fluorescence. PI is a nuclear counterstain, which enters cells with compromised plasma membrane and emits red fluorescence. Therefore, the number of PI and NucBlue stained cells provides the count of dead and total number (dead or alive) of cells, respectively. NucBlue and PI positive cells were observed with a 40× dry objective using appropriate filters and counted using ImageJ software. The data were analyzed and plotted using GraphPad prism.

Statistical Analysis. After spectral normalization, Raman intensities obtained at different wavenumbers from each cell were further normalized to the initial or before value measured from the same cell when the latter was set to 100 at the respective wavenumber. All the data are presented as mean ± SEM. Time dependent changes in the peak intensities were tested using repeated measures one-way ANOVA, followed by multiple comparisons using Newman−Keuls test as required. The differences between two groups were compared using two-way repeated measures ANOVA. Multiple comparisons at each time point were performed by Bonferroni post-test as required. In this study, differences were evaluated at three levels of significance: $P < 0.05$, $P < 0.01$, and $p < 0.001$ indicated by the symbols *, #, and $, respectively.

■ ASSOCIATED CONTENT

Supporting Information

The Supporting Information is available free of charge on the ACS Publications website at DOI: 10.1021/acschemneuro.5b00106.

Bar graphs describing the time dependent changes in the intensity of DNA related peaks in only $FeSO_4$, only H_2O_2, control, oxidatively stressed, only ascorbate, and ascorbate cotreated group (PDF)

■ AUTHOR INFORMATION

Corresponding Authors

*Tel: 91-80-22932595. Fax: 91-80-23601552. E-mail: umapathy@ipc.iisc.ernet.in.

*Tel: 91-80-22933220. Fax: 91-80-23600535. E-mail: sks@mbu.iisc.ernet.in.

Author Contributions

A.D. designed, performed the experiments, analyzed the data completely, and wrote the manuscript. R.G. contributed to preliminary Raman spectroscopy experiments and part of the data analysis. S.C. supplied the cell culture and fluorescence data analysis. F.A. reviewed and edited the manuscript. S.K.S. and S.U. supervised the work. All the authors read and edited the manuscript.

Funding

This work is financially supported by Department of Biotechnology, Govt. of India.

Notes

The authors declare no competing financial interest.

■ ACKNOWLEDGMENTS

A.D. is thankful to DBT postdoctoral program.

■ REFERENCES

(1) Gilgun-Sherki, Y., Melamed, E., and Offen, D. (2001) Oxidative stress induced-neurodegenerative diseases: the need for antioxidants that penetrate the blood brain barrier. *Neuropharmacology 40*, 959−975.

(2) Emerit, J., Edeas, M., and Bricaire, F. (2004) Neurodegenerative diseases and oxidative stress. *Biomed. Pharmacother. 58*, 39−46.

(3) Gough, D. R., and Cotter, T. G. (2011) Hydrogen peroxide: a Jekyll and Hyde signaling molecule. *Cell Death Dis. 2*, e213.

DOI: 10.1021/acschemneuro.5b00106
ACS Chem. Neurosci. 2015, 6, 1794−1801

(4) Chang, W. T., Lin, H. L., Chen, H. C., Wu, Y. M., Chen, W. J., Lee, Y. T., and Liau, I. (2009) Real-time molecular assessment on oxidative injury of single cells using Raman spectroscopy. *J. Raman Spectrosc. 40*, 1194−1199.
(5) Henle, E., Han, Z., Tang, N., Rai, P., Luo, Y., and Linn, S. (1999) Sequence-specific DNA cleavage by Fe^{2+}- mediated Fenton reactions has possible biological implications. *J. Biol. Chem. 274*, 962−971.
(6) Baumeister, P., Huebner, T., Reiter, M., Schwenk, Z. S., and Harreus, U. (2009) Reduction of oxidative DNA fragmentation by ascorbic acid, zinc and *N*-acetylcysteine in nasal mucosa tissue cultures. *Anticancer Res. 29*, 4571−4574.
(7) Nakamura, J., Purvis, E. R., and Swenberg, J. A. (2003) Micromolar concentrations of hydrogen peroxide induce oxidative DNA lesions more efficiently than millimolar concentrations in mammalian cells. *Nucleic Acids Res. 31* (6), 1790−1795.
(8) Zhu, D., Kevin, S., Tan, K. S., Zhang, X. X., Sun, A. Y., Sun, G. Y., and Lee, J. C.M. (2005) Hydrogen peroxide alters membrane and cytoskeleton properties and increases intercellular connections in Astrocytes. *J. Cell Sci. 118*, 3695−3703.
(9) Hyslop, P. A., Zhang, Z., Pearson, D. V., and Phebus, L. A. (1995) Measurement of striatal H_2O_2 by microdialysis following global forebrain ischemia and reperfusion in the rat: correlation with the cytotoxic potential of H_2O_2 in vitro. *Brain Res. 671*, 181−186.
(10) Terashvili, M., Sarkar, P. A., Nostrand, M. V., Falck, J. R., and Harder, D. R. (2012) The protective effect of astrocyte-derived 14, 15-epoxyeicosatrienoic acid on hydrogen Peroxide-induced cell injury in astrocyte-dopaminergic Neuronal cell line co-culture. *Neuroscience 223*, 68−76.
(11) Kim, E. J., Won, R., Sohn, J. H., Chung, M. A., Nam, T. S., Lee, H. J., and Lee, B. H. (2008) Anti-oxidant effect of ascorbic and dehydroascorbic acids in hippocampal slice culture. *Biochem. Biophys. Res. Commun. 366*, 8−14.
(12) Singh, B., Gautam, R., Kumar, S., Vinay Kumar, B. N., Nongthomba, U., Nandi, D., Mukherjee, G., Santosh, V., Somasundaram, K., and Umapathy, S. (2011) Application of vibrational microspectroscopy to biology and medicine. *Curr. Sci. 102*, 232−244.
(13) Lloyd, G., Almond, L. M., Stone, N., Shepherd, N., Sanders, S., Hutchings, J., Barr, H., and Kendall, C. (2014) Utilising non-consensus pathology measurements to improve the diagnosis of oesophageal cancer using a Raman spectroscopic probe. *Analyst 139*, 381−388.
(14) Gautam, R., Vanga, S., Madan, A., Nongthomba, U., and Umapathy, S. (2015) Raman Spectroscopic Studies on Screening of Myopathies. *Anal. Chem. 87*, 2187−2194.
(15) Gautam, R., Samuel, A., Sil, S., Chaturvedi, D., Dutta, A., Ariese, F., and Umapathy, S. (2015) Raman and Infrared Imaging: Applications and Advancements. *Curr. Sci. 108*, 341−356.
(16) Kumar, S., Matange, N., Umapathy, S., and Visweswariah, S.-S. (2015) Linking carbon metabolism to carotenoid production in mycobacteria using Raman spectroscopy. *FEMS Microbiol. Lett. 362*, 1−6.
(17) Krafft, C., Knetschke, T., Funk, R., and Salzer, R. (2006) Studies on Stress-Induced Changes at the Subcellular Level by Raman Microspectroscopic Mapping. *Anal. Chem. 78*, 4424−4429.
(18) Sanchez, V., Redmann, K., Wistuba, J., Wübbeling, F., Burger, M., Oldenhof, H., Wolkers, W. F., Kliesch, S., Schlatt, S., and Mallidis, C. (2012) Oxidative DNA damage in human sperm can be detected by Raman microspectroscopy. *Fertil. Steril. 98*, 1124−1129.
(19) Notingher, I., Green, C., Dyer, C., Perkins, E., Hopkins, N., Lindsay, C., and Hench, L. L. (2004) Discrimination between ricin and sulphur mustard toxicity in vitro using Raman spectroscopy. *J. R. Soc., Interface 1*, 79−90.
(20) Notingher, I., Selvakumaran, J., and Hench, L. L. (2004) New detection system for toxic agents based on continuous spectroscopic monitoring of living cells. *Biosens. Bioelectron. 20*, 780−789.
(21) Yao, H., Tao, Z., Ai, M., Peng, L., Wang, G., He, B., and Li, Y. Q. (2009) Raman spectroscopic analysis of apoptosis of single human gastric cancer cells. *Vib. Spectrosc. 50*, 193−197.
(22) Owen, C. A., Selvakumaran, J., Notingher, I., Jell, G., Hench, L. L., and Stevens, M. M. (2006) In Vitro Toxicology Evaluation of Pharmaceuticals Using Raman Micro-Spectroscopy. *J. Cell. Biochem. 99*, 178−86.
(23) Brauchle, E., Thude, S., Brucker, S. Y., and Schenke-Layland, K. (2014) Cell death stages in single apoptotic and necrotic cells monitored by Raman microspectroscopy. *Sci. Rep. 4*, 4698.
(24) Bankapur, A., Krishnamurthy, R.-S., Zachariah, E., Santhosh, C., Chougule, B., Praveen, B., Valiathan, M., and Mathur, D. (2012) Micro-Raman Spectroscopy of Silver Nanoparticle Induced Stress on Optically-Trapped Stem Cells. *PLoS One 7*, e35075.
(25) Ghita, A., Pascut, F. C., Mather, M., Sottile, V., and Notingher, I. (2012) Cytoplasmic RNA in Undifferentiated Neural Stem Cells: A Potential Label-Free Raman Spectral Marker for Assessing the Undifferentiated Status. *Anal. Chem. 84*, 3155−3162.
(26) Giordano, G., and Costa, L. G. (2011) Primary Neurons in Culture and Neuronal Cell Lines for In Vitro Neurotoxicological Studies. In Vitro Neurotoxicology. *Methods Mol. Biol. 758*, 13−27.
(27) Schenck, J. F. (2010) MRI of brain iron and neurodegenerative diseases, a potential biomarker. In *Iron deficiency and overload: From basic biology to clinical medicine* (Yehuda, S., and Mostofsky, D. I., Eds.), page 229, Chapter 13, Humana Press, Springer, New York.
(28) Kim, N. H., Park, S. J., Jin, J. K., Kwon, M. S., Choi, E. K., Carp, R. I., and Kim, Y. S. (2000) Increased ferric iron content and iron-induced oxidative stress in the brains of scrapie-infected mice. *Brain Res. 884*, 98−103.
(29) Alcântara, D. D. F. A., Ribeiro, H. F., Matos, L. A., Sousa, J. M. C., Burbano, R. R., and Bahia, M. O. (2013) Cellular responses induced in vitro by iron (Fe) in a central nervous system cell line (U343MGa). *GMR, Genet. Mol. Res. 12*, 1554−1560.
(30) Liu, R., Liu, W., Doctrow, S. R., and Baudry, M. (2003) Iron toxicity in organotypic cultures of hippocampal slices:role of reactive oxygen species. *J. Neurochem. 85*, 492−502.
(31) Hardaway, C. M., Badisa, B., and Soliman, K. F. A. (2012) Effect of ascorbic acid and hydrogen peroxide on mouse neuroblastoma cells. *Mol. Med. Rep. 5*, 1449−1452.
(32) Huang, H., Shi, H., Feng, S., Chen, W., Yu, Y., Lin, D., and Chen, R. (2013) Confocal Raman spectroscopic analysis of the cytotoxic response to cisplatin in nasopharyngeal carcinoma cells. *Anal. Methods 5*, 260−266.
(33) Moritz, T. J., Taylor, D. S., Krol, D. M., Fritch, J., and Chan, J. W. (2010) Detection of doxorubicin-induced apoptosis of leukemic T-lymphocytes by laser tweezers Raman spectroscopy. *Biomed. Opt. Express 1*, 1138−1147.
(34) Ren, J. G., Xia, H. L., Just, T., and Dai, Y. R. (2001) Hydroxyl radical-induced apoptosis in human tumor cells is associated with telomere shortening but not telomerase inhibition and caspase activation. *FEBS Lett. 488*, 123−132.
(35) Suematsu, N., Hosoda, M., and Fujimori, K. (2011) Protective effects of quercetin against hydrogen peroxide-induced apoptosis in human neuronal SH-SY5Y cells. *Neurosci. Lett. 504*, 223−227.
(36) Lu, W. C., Chen, C. J., Hsu, H. C., Hsu, H. L., and Chen, L. (2010) The adaptor protein SH2B1β reduces hydrogen peroxide-induced cell death in PC12 cells and hippocampal neurons. *J. Mol. Signaling 5*, 17.
(37) Kooncumchoo, P., Sharma, S., Porter, J., Govitrapong, P., and Ebadi, M. (2006) Coenzyme Q_{10} Provides Neuroprotection in Iron-Induced Apoptosis in Dopaminergic Neurons. *J. Mol. Neurosci. 28*, 125−141.
(38) Gautam, D. K., Misro, M., Chaki, S. K., and Sehgal, N. (2006) H_2O_2 at physiological concentrations modulates Leydig cell function inducing oxidative stress and apoptosis. *Apoptosis 11*, 39−46.
(39) Ammar, D. A., Hamweyah, K. M., and Kahook, M. Y. (2012) Antioxidants Protect Trabecular Meshwork Cells From Hydrogen Peroxide-Induced Cell Death. *TVST. 1*, 4.

DOI: 10.1021/acschemneuro.5b00106
ACS Chem. Neurosci. 2015, 6, 1794−1801